

000
001
002
003

LEARNING TO EVICT FROM KEY-VALUE CACHE

004
005
006
007
008
009010 **Anonymous authors**
011
012
013
014
015
016
017
018
019
020
021
022
023
024
025
026
027
028
029
030
031
032
033
034
035
036
037
038
039
040
041
042
043
044
045
046
047
048
049
050
051
052
053040 Paper under double-blind review
041
042
043
044
045
046
047
048
049
050
051
052
053

ABSTRACT

The growing size of Large Language Models (LLMs) makes efficient inference challenging, primarily due to the memory demands of the autoregressive Key-Value (KV) cache. Existing eviction or compression methods reduce cost but rely on heuristics, such as recency or past attention scores, which serve only as indirect proxies for a token’s future utility and introduce computational overhead. We reframe KV cache eviction as a reinforcement learning (RL) problem: learning to rank tokens by their predicted usefulness for future decoding. To this end, we introduce KV Policy (KVP), a framework of lightweight per-head RL agents trained on pre-computed generation traces using only key and value vectors. Each agent learns a specialized eviction policy guided by a holistic reward, derived from future utility, that evaluates the quality of the ranking across all cache budgets, requiring no modifications to the underlying LLM or additional inference. Evaluated on the long-context benchmark RULER and the multi-turn dialogue benchmark OASST2-4k, KVP significantly outperforms baselines. Furthermore, zero-shot tests on standard downstream tasks indicate that KVP generalizes well beyond its training distribution. These results demonstrate that learning to predict future token utility is a powerful and scalable paradigm for adaptive KV cache management.

1 INTRODUCTION

Large Language Models (LLMs) based on the Transformer architecture (Vaswani et al., 2017) have revolutionized natural language processing, demonstrating remarkable capabilities across a wide range of tasks (Brown et al., 2020; Önden & Alnour, 2023; Touvron et al., 2023). However, their practical deployment, especially for applications involving long sequences or interactive sessions, is often burdened by substantial computational requirements during inference. A critical bottleneck arises from the Key-Value (KV) cache, a mechanism inherent to autoregressive generation in Transformers (Sheng et al., 2023). This cache stores the keys and values of previous tokens, avoiding redundant computations but growing linearly with the input and generated sequence length. For long contexts, the KV cache can consume tens or even hundreds of gigabytes of memory, rapidly exceeding the capacity of modern hardware accelerators and necessitating strategies for efficient management.

To address this memory challenge, a variety of KV cache management techniques have been proposed. These range from simple heuristics like keeping only the most recent tokens (sliding window), to more sophisticated methods that leverage insights into attention patterns. Approaches like H2O, SnapKV, and TOVA Zhang et al. (2023); Li et al. (2024); Oren et al. (2024) use signals such as past attention scores or attention sinks to identify and retain important tokens. Others employ quantization to reduce the memory footprint (Dettmers et al., 2022; Xiao et al., 2023) or use low-rank approximations to represent the cache state more compactly (Singhania et al., 2024; Ribar et al., 2024).

While these hand-crafted policies have advanced the state of the art, they are fundamentally built on heuristics that serve as indirect proxies for a token’s future importance. They assume that what was important before will remain important. This assumption might not always hold, as the informational needs of generation are dynamic and content-dependent. A token’s true value is determined by its utility to future decoding steps, a quantity these methods do not directly optimize for. Consequently, they are prone to suboptimal eviction decisions, leading to an irrecoverable loss of critical information and degraded generation quality. Even post-hoc compression methods based on attention signals are fundamentally backward-looking and have additional drawbacks: they require repeated computation of attention statistics, which introduces significant overhead; and they are not compatible with efficient implementations like FlashAttention (Dao et al., 2022), limiting their practicality.

| | KVP | Future Attention Importance | StreamingLLM |
|-----|---|---|---|
| 054 | I'm planning a trip to Rome next month. I want to visit the Colosseum, the Vatican Museums, and the Trevi Fountain. What's the best order to visit these attractions to minimize travel time? < im_end > Also, should I book tickets in advance for these places?< im_end > | I'm planning a trip to Rome next month. I want to visit the Colosseum, the Vatican Museums, and the Trevi Fountain. What's the best order to visit these attractions to minimize travel time? < im_end > Also, should I book tickets in advance for these places?< im_end > | I'm planning a trip to Rome next month. I want to visit the Colosseum, the Vatican Museums, and the Trevi Fountain. What's the best order to visit these attractions to minimize travel time? < im_end > Also, should I book tickets in advance for these places?< im_end > |

058 **Figure 1: Future token importance for KV cache eviction.** Effective KV cache eviction requires
 059 identifying tokens that will receive little or no future attention. (*center*) We roll out a sample KV cache
 060 and measure the true cumulative future attention for each token, then rank tokens by this importance
 061 and color them accordingly (bright = high rank, white = low). (*right*) Importance estimated by
 062 the fixed sink-and-recency heuristic of *StreamingLLM* deviates substantially from true importance
 063 ranking. (*left*) Our learned policy closely recovers the complex, non-local structure of future attention
 064 despite using only past keys and values, without access to queries, attention scores, or future tokens.
 065 *We expand the comparison with all strategies in Figure 7.*

066
 067 In this work, we move beyond hand-crafted policies and reframe KV cache eviction as a Reinforce-
 068 ment Learning (RL) problem: learning an attention-free policy that selects which tokens to evict. We
 069 formulate this learning problem as a ranking task, where the agent orders tokens by their predicted
 070 future utility. As qualitatively illustrated in Figure 1, a learned policy can successfully approximate a
 071 token’s future utility, a complex, non-local structure, where simple heuristics fail. Such a ranking
 072 enables a highly efficient and flexible strategy: eviction is performed by discarding the lowest-ranked
 073 entries to meet any memory budget. As a reward signal, we define the ranking successful if for any
 074 given cache size, the most valuable information is retained, thus minimizing performance degradation.
 075

076 We introduce KV Policy (KVP), a framework that trains a distinct, lightweight RL agent for each
 077 KV head in the model. This per-head specialization allows each policy to adapt to the unique
 078 attentional patterns of its corresponding head. The agents are trained efficiently on pre-computed
 079 generation traces without any additional inference, using only the key and value vectors as input
 080 and requiring no architectural changes to the underlying LLM. To train the agents, we introduce a
 081 reward that holistically evaluates the quality of the policy’s sorting for all possible cache budgets.
 082 For every possible cache budget, we measure how much essential information in the future would be
 083 erroneously evicted with the candidate sorting when only the top tokens from the cache are kept.

084 Evaluated on long-context synthetic benchmark RULER (Hsieh et al., 2024) and a multi-turn natural
 085 language benchmark OASST2-4k (Köpf et al., 2023), KVP significantly outperforms strong heuristic
 086 baselines, demonstrating that learning specialized policies to predict the future utility of tokens is
 087 a powerful and scalable paradigm for KV cache eviction. Evaluation in a zero-shot generalization
 088 setting on standard downstream benchmarks from the EleutherAI Language Model Evaluation
 089 Harness (Gao et al., 2024) suggests that KVP retains strong performance even out of distribution.

090 In summary, our main contributions are:

- 091 • We reframe KV cache eviction as a learning problem: ranking cache entries by their predicted
 092 future utility.
- 093 • We introduce KVP, a system of lightweight, per-head RL agents that learn specialized
 094 sorting policies using only key and value vectors without using any attention information.
- 095 • We propose a holistic reward that evaluates eviction policies across all cache budgets without
 096 additional LLM inference.
- 097 • We show that KVP substantially improves long-context performance over strong baselines
 098 and generalizes to unseen domains.

101 2 RELATED WORK

102 **Attention-Based Eviction.** Eviction-based approaches aim to choose a subset of the KV cache.
 103 Early methods used simple heuristics like First-In-First-Out (FIFO) or Least Recently Used (LRU)
 104 (Xiao et al., 2024). More recent work leverages the inherent sparsity in attention patterns. Techniques
 105 like StreamingLLM (Xiao et al., 2024) and H2O (Zhang et al., 2023) observe that initial tokens
 106 (“attention sinks”) and recent tokens often capture most of the required context, allowing for the
 107 eviction of intermediate tokens. Others, such as KeyFormer (Adnan et al., 2024) and related works

(Cai et al., 2024), explicitly analyze attention scores or structures to identify and retain important tokens, sometimes using the current query to inform eviction (Li et al., 2024; Lee et al., 2024a). Although our work is an eviction methodology, it departs from this paradigm by instead learning a *forward-looking, query-independent policy* to directly predict a token’s future utility, rather than inferring it from past attention or the current query.

Memory Hierarchy Management. Recognizing the limited size of fast GPU memory, some approaches utilize system memory (CPU RAM) as a secondary cache layer (Chen et al., 2024b; Sheng et al., 2023). Recent sparse retrieval approaches, such as IceCache (Anonymous, 2025), ArkVale (Chen et al., 2024a), MagicPig (Chen et al., 2025), and InfiniGen (Lee et al., 2024b), manage these hierarchies by offloading KV entries to slower memory and retrieving them only when needed, possibly in pages (Tang et al., 2024). While this allows for effectively larger cache sizes, it introduces significant latency (a reload cost) when accessing offloaded entries. Policies for deciding what and when to offload are often heuristic. While our work focuses on eviction, the learned ranking it produces provides a principled, data-driven signal for such hierarchical management: the lowest-ranked entries are natural candidates for being moved to slower memory, representing a powerful synergy between our approaches.

Representation Compression. Instead of removing entries, another line of work focuses on reducing the memory required per entry. Quantization techniques reduce the numerical precision (e.g., to 8-bit integers or lower) of keys and values, significantly cutting memory usage, often with minimal performance impact (Dettmers et al., 2022; Xiao et al., 2023), while low-rank approximation methods represent the key and value matrices using lower-dimensional projections (Singhania et al., 2024; Ribar et al., 2024). A distinct approach is state merging, where methods like MorphKV (Ghadia et al., 2025) identify and combine semantically similar KV pairs into new, synthetic representations. These techniques are orthogonal and complementary to eviction strategies, as one could utilize our approach to filter out the least useful tokens and then apply MorphKV’s merging logic to the remaining high-utility tokens.

Learned Approaches. Applying machine learning to directly optimize cache management policies is less common than heuristic approaches. While learning has been used extensively for general caching problems (Afrin et al., 2024; Shuja et al., 2020; Wang & Friderikos, 2020), its application specifically to the dynamic nature of the Transformer KV cache is emerging (Chari et al., 2025; Cetin et al., 2024; Nawrot et al., 2024; Ge et al., 2024). Some recent works, such as Gisting Token (Deng et al., 2025) and Activation Beacon (Zhang et al., 2025), learn to compress context into compact summary tokens or condensed activations. Our work differs by learning a fine-grained ranking over all tokens rather than a summary; however, these approaches are complementary, as KVP could identify which tokens are best suited for summarization. Our approach is distinguished by utilizing RL to train a lightweight, per-head policy. A novel reward signal, the eviction error across all cache budgets, ensures robust performance under varying memory limits. Furthermore, the per-head rankings and future attention estimates from KVP could directly inform a dynamic, non-uniform budget allocation, a promising direction for future work.

Overall, while prior work has addressed KV cache constraints through heuristics, memory hierarchies, or compression, our approach introduces an RL framework that casts eviction as a ranking problem. By training lightweight, per-head policies to predict tokens’ future utility and optimizing them with a global, budget-agnostic reward, we offer an adaptive, query-independent solution. Crucially, this method is also complementary to many existing techniques, and may provide a principled signal for memory offloading, context gisting, or dynamic budget allocation.

3 METHODOLOGY: LEARNING TO EVICT KV CACHE ENTRIES

We consider the problem of KV cache eviction: given n tokens $\mathcal{X} = \{x_i\}_{i \in [n]}$ and a budget b , select a subset $\mathcal{S}^* \subset \mathcal{X}$ maximizing some downstream performance reward R as

$$\mathcal{S}_b^* \in \arg \max_{|\mathcal{S}|=b, \mathcal{S} \subset \mathcal{X}} R(\mathcal{S}). \quad (1)$$

Because generation is autoregressive and budgets vary over time, a practical solution must handle arbitrary n and all $b \in [n]$. Although this selection problem is NP-hard even for linear rewards (Nemhauser et al., 1978), it becomes structured under two mild conditions: **(i) uniqueness:**

162 each S_b^* is unique and **(ii) nestedness**: $S_b^* \subset S_{b+1}^*$ for all b . Uniqueness can be straightforwardly
 163 achieved with simple tie-breaking and nestedness is natural because tokens essential under a small
 164 budget should remain so as capacity grows. Under these constraints KV cache eviction problem is
 165 equivalent to KV cache ranking *with proof deferred to Appendix A.1*.

166 **Proposition 1.** *Assume (i) uniqueness of each S_b^* and (ii) nestedness: $S_b^* \subset S_{b+1}^*$ for all b . Then,
 167 there exists a total order (ranking) π such that*

$$169 \quad S_b^* = \{i \in [n] : \pi(i) \leq b\} \quad \text{for all } b.$$

170 *Equivalently, there exists a scoring function whose top- b elements realize S_b^* for every b .*

171 Proposition 1 lets us reformulate eviction as learning a single budget-agnostic scoring function. At
 172 any generation step, the cache entries are ordered from most to least valuable for future decoding
 173 using the learned scoring function; for a given budget b , we retain the top- b . A high-quality ranking
 174 preserves critical information across all budgets, minimizing degradation.

175 To learn this scoring function, we adopt a reinforcement-learning (RL) approach. We parameterize
 176 a stochastic ranking policy and directly optimize the true discrete end-to-end reward using policy-
 177 gradient methods. We later analyze this choice against differentiable relaxations of sorting (Prillo &
 178 Eisenschlos, 2020; Grover et al., 2019; Blondel et al., 2020) in Section 4.3.

179 We employ a lightweight RL agent, governed by parameters θ , to define the scoring function $f(\cdot; \theta)$.
 180 To capture the specialized functions of different attention mechanisms, we train a distinct agent for
 181 each KV head in the LLM. To this end, we introduce KVP, a framework for efficiently training
 182 lightweight, per-head RL agents to perform this ranking. In the remaining of this section, we first
 183 discuss the agent architecture, then the reward, and finally the learning process.

187 3.1 KV CACHE EVICTION AGENT

188 In order to formulate learning to sort as an RL problem, we largely follow the Plackett-Luce model
 189 (Plackett, 1975). Given a set of input tokens $\{x_i\}_{i \in [N]}$, we learn a parametric scoring function
 190 $f(x_i; \theta)$ which assigns a score to each input token x_i . This scoring function induces a stochastic
 191 sorting policy π_θ which samples permutation $\sigma = (\sigma_1, \dots, \sigma_N)$ sequentially as;

$$193 \quad \pi_\theta(\sigma|x_1, \dots, x_N) = \prod_{i=1}^N \frac{\exp(f(x_{\sigma_i}; \theta))}{\sum_{j=i}^N \exp(f(x_{\sigma_j}; \theta))} \quad (2)$$

194 At each step i , the next element σ_i is sampled proportionally to its score, normalized over the
 195 remaining tokens. This process defines a valid distribution over all permutations. The scoring
 196 function $f(\cdot; \theta)$ together with the sampling policy, forms our KV cache eviction agent. We next
 197 specify the parameterization of $f(\cdot; \theta)$.

198 **Scoring Function** The representation for token x_i is the concatenation of its key vector k_i , value
 199 vector v_i , and its original position pos_i as $x_i = (k_i, v_i, pos_i)$. We define the scoring function $f(\cdot; \theta)$
 200 as a small Multi-Layer Perceptron (MLP) parametrized with θ as $f(x_i; \theta) = MLP_\theta(k_i, v_i, pos_i)$.
 201 Crucially, the policy relies only on information available in the cache and does not require access to
 202 future information, previous attention scores or any query embedding.

203 **Efficient Parallel Sampling with Gumbel-Sort** While Equation (2) defines the distribution,
 204 sequential sampling is inefficient. Fortunately, a permutation can be sampled from this distribution in
 205 a single step using the Gumbel-Sort (Mena et al., 2018). Given the scores $f(x_i; \theta)$, we generate i.i.d.
 206 noise samples $g_i \sim \text{Gumbel}(0, 1)$. A permutation σ is then sampled by sorting the perturbed scores:

$$207 \quad \sigma = \text{argsort}_{i \in [N]} (f(x_i; \theta) + g_i) \quad (3)$$

208 This procedure is non-autoregressive, fully parallelizable on modern hardware, and allows us to
 209 sample an entire permutation with just one forward pass of the scoring model and a fast sort operation.
 210 This is critical for efficient training.

216 3.1.1 GLOBAL REWARD FOR OFFLINE RL
217

218 A key component of our framework is a reward signal that globally evaluates the quality of an
219 agent’s entire ranked output, directly optimizing for the efficient preservation of information across all
220 possible cache budgets. More importantly we define this reward in a way to enable training without
221 any additional LLM inference.

222 Consider the input set of n tokens $\mathcal{X} = \{x_i\}_{i \in [n]}$ and a candidate permutation $\{\sigma_i\}_{i \in [n]}$, ordered
223 from most to least important. The total reward is defined as the sum of reward over all possible target
224 cache sizes $1 \leq b \leq n - 1$. Since the kept tokens are always the top- b , this translates into
225

$$226 \quad \mathcal{R}(\sigma_1, \dots, \sigma_n; \mathcal{X}) = \sum_{b=1}^{n-1} \mathcal{R}^b(\sigma_{n-b}, \dots, \sigma_n; \mathcal{X}) \quad (4)$$

229 where \mathcal{R}^b is the reward for a specific budget b .
230

231 We define \mathcal{R}^b based on an importance score derived from the future attention patterns. Consider f
232 future tokens (x_{n+1} to x_{n+f}) in the training data after n input tokens and the attention as $A(x_i, x_j)$,
233 we define the importance of token x_i as the total future attention it accumulates: $\sum_{j=n+1}^{n+f} A(x_i, x_j)$.
234

235 Given the permutation σ , a cache of budget b retains the top- b tokens $\sigma_1, \dots, \sigma_b$ and evicts the rest.
236 The cost for this budget is the total importance of the evicted tokens. We define the per-budget reward
237 \mathcal{R}^b as the negative of this cost for all evicted tokens:
238

$$239 \quad \mathcal{R}^b(\sigma_1, \dots, \sigma_n; \mathcal{X}) = - \sum_{i=b+1}^n \sum_{j=n+1}^{n+f} A(x_{\sigma_i}, x_j) \quad (5)$$

242 For models with Grouped-Query Attention (Ainslie et al., 2023), the attention score $A(x_i, x_j)$ from a
243 future query group is the maximum attention value across all queries within that group.
244

245 To create an objective invariant to scale and attention scores distribution, we normalize the total
246 cost by the cost incurred by an optimal ranking σ^* . The final reward we optimize is normalized as
247 $\mathcal{R}(\sigma_1, \dots, \sigma_n; \mathcal{X}) / \mathcal{R}(\sigma_1^*, \dots, \sigma_n^*; \mathcal{X})$. In the experimental section, when we refer directly to \mathcal{R}^b , we always
248 refer to its normalized version $\mathcal{R}^b(\sigma_1, \dots, \sigma_n; \mathcal{X}) / \mathcal{R}(\sigma_1^*, \dots, \sigma_n^*; \mathcal{X})$.
249

250 3.2 PER-HEAD RL AGENT AND EFFICIENT TRAINING
251

252 A significant advantage of our method is its training efficiency. The agents are trained entirely offline,
253 obviating the need for live LLM inference within the RL optimization loop. This is due to the fact
254 that our usefulness score is function of true sequences, not generated sequences. First, we generate a
255 dataset by running the base LLM on a training corpus. For each sample, we store the full sequence of
256 queries, keys, and values. The attention matrices are not stored due to their prohibitive size.
257

258 During training, we sample a sequence and a cache size to be evicted from. We update the parameters
259 θ of the agent using a policy gradient algorithm. Since our reward $\mathcal{R}(\sigma)$ is a terminal reward assigned
260 only after the entire permutation σ is generated, the objective is $J(\theta) = \mathbb{E}_{\sigma \sim \pi_\theta} [\mathcal{R}(\sigma)]$. We use the
261 REINFORCE algorithm with a Leave-One-Out (RLOO) baseline (Williams, 1992; Ahmadian et al.,
262 2024) to reduce variance. For an episode (permutation) σ^k within a batch of K episodes, the baseline
263 $\bar{\mathcal{R}}$ is the average terminal reward of all other episodes in the batch. Considering the advantage,
264 $\mathcal{R}(\sigma^k) - \bar{\mathcal{R}}$, the gradient is thus estimated as:
265

$$266 \quad \nabla_\theta J(\theta) \approx \frac{1}{K} \sum_{k=1}^K \left[(\mathcal{R}(\sigma^k) - \bar{\mathcal{R}}) \sum_{i=1}^n \nabla_\theta \log \pi_\theta(\sigma_i^k | \mathcal{X}) \right]. \quad (6)$$

267 We summarize the training in Alg. 1 and defer the further implementation details to Appendix A.2.
268

269 Training per-head agents from offline traces is highly scalable. At inference, the learned policy for
each head ranks its KV entries, and the trailing entries are evicted based on the budget.

270 Algorithm 1 RL Training Loop on Pre-Computed KV Traces

271 1: **Input:** Static dataset of pre-computed traces over m sequences each with length $n_j, j \in [m]$
 272 denoted as $\mathcal{X}^j = \{x_i^j\}_{i \in n_j}$ containing Q, K, V tensors.
 273 2: **while** training not converged **do**
 274 3: Sample a data item $j \sim \text{Unif}(m)$ and a cache size $n \sim \text{Unif}(n_j)$.
 275 4: Sample K permutations from the agent $\sigma_1^k, \dots, \sigma_n^k \sim \pi_\theta(\sigma | x_1^j, \dots, x_n^j), k \in [K]$
 276 5: Calculate reward $\mathcal{R}(\sigma_1^k, \dots, \sigma_n^k; \mathcal{X}^j)$ using equation 4.
 277 6: Update θ using equation 6.
 278 7: **end while**

280
281 **4 EVALUATION**
282

283 We hypothesize that a high-quality KV cache eviction policy can be trained entirely offline and
 284 deployed at inference time using only static token features (keys, values, and positions). To validate
 285 this, we conduct a comprehensive evaluation of KVP across multiple language modeling bench-
 286 marks and a wide range of cache budgets. Our results show that KVP consistently shows stronger
 287 downstream performance relative to existing heuristics, including methods that exploit privileged,
 288 query-specific information. We also provide ablation studies to analyze the design choices that enable
 289 this performance.

290
291 **4.1 EXPERIMENTAL SETUP**
292

293 **Base Model and Datasets.** Our experimental setup is centered on the *Qwen2.5-7B-Chat* model
 294 (Yang et al., 2024; Wang et al., 2024), a state-of-the-art transformer LLM. Please refer to Figure 6 in
 295 the Appendix for additional experiment on *Phi-4 14B* (Abdin et al., 2025). We train and evaluate
 296 our KVP agents using two distinct long-context benchmarks: *RULER-4k* (Hsieh et al., 2024), a
 297 synthetic dataset designed to probe long-context reasoning with sequences of approximately 4500
 298 tokens; and *OASST2-4k*, a curated subset of the OpenAssistant Conversations Dataset (Köpf et al.,
 299 2023) featuring multi-turn dialogues of similar length. To assess generalization, we further perform
 300 zero-shot evaluation on four standard downstream benchmarks from the EleutherAI Language Model
 301 Evaluation Harness (Gao et al., 2024): *BoolQ* (Clark et al., 2019), a reading comprehension task
 302 framed as yes/no question answering; *ARC-Challenge* (Clark et al., 2018), a collection of science
 303 exam questions requiring multi-step reasoning; *MMLU* (Hendrycks et al., 2021), a benchmark
 304 testing expert-level knowledge across a wide range of domains; *HellaSwag* (Zellers et al., 2019), a
 305 commonsense sentence completion task; and *GovReport* (Bai et al., 2023), a summarization task
 306 from the LongBench benchmark for long context understanding. Importantly, KVP is not trained or
 307 fine-tuned on these tasks. Please refer to Appendix A.2 for further implementation details.

308 **Baselines.** We benchmark KVP against two main categories of KV cache management techniques:
 309 attention-based and attention-free. The first category includes state-of-the-art methods like *TOVA*
 310 (Oren et al., 2024) and *SnapKV* (Li et al., 2024). These methods leverage attention scores to identify
 311 important tokens, which introduces computational overhead by tying the eviction strategy to the
 312 attention calculation step. The second, more efficient category of attention-free baselines, to which
 313 our own KVP agents belong, operates independently of the attention mechanism. This group includes
 314 a *Random* eviction baseline, the recency-based *StreamingLLM* (Xiao et al., 2024), and several
 315 approaches that prune tokens based on their key embeddings. These include methods based on
 316 statistical patterns (*LagKV* (Liang et al., 2025)), vector similarity (*KeyDiff* (Park et al., 2025)), and
 317 L2 norm (*K-Norm* (Devoto et al., 2024)). To ensure a fair comparison, we adapt all baselines to our
 318 ranking-based framework by converting their binary keep/evict decisions into a full token permutation,
 319 enabling evaluation with consistent metrics.

320 **Budgeting and Compression Schedule.** For all online evaluations, we follow a consistent com-
 321 pression protocol. First, the entire context, including the final user message or question that prompts
 322 the generation, is processed by the LLM to populate the initial KV cache (the “prefill” stage). Second,
 323 the specified compression method is applied to this pre-populated cache to reduce its size to the target
 budget. Finally, the model generates the response autoregressively using the compressed cache. This

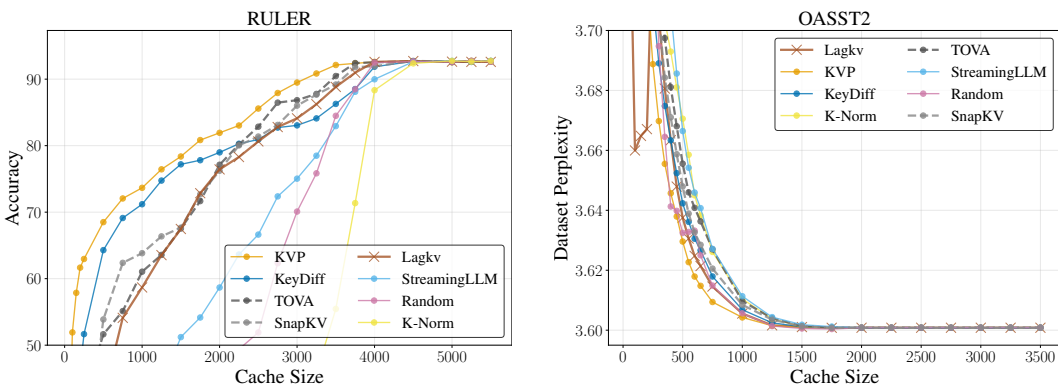
324 setup tests the ability to compress a large context before generation begins. To isolate the performance
 325 of the core ranking strategy, we apply a uniform compression budget across all heads and layers for
 326 all methods. This ensures a fair comparison focused purely on the quality of the eviction strategy
 327 itself, rather than on budget allocation heuristics. While head-specific or layer-specific budgeting is
 328 an orthogonal and promising direction for further performance improvements, our approach provides
 329 a clear and interpretable evaluation of the underlying policies.

330
 331 **Inference Efficiency.** Our KVP agents make their ranking decisions using only the Key and Value
 332 vectors, and their position in the context. This makes KVP highly efficient, as it avoids re-computing
 333 attention scores. In contrast, attention-based baselines like TOVA and SnapKV are evaluated using
 334 the attention scores generated during the prefill stage, giving them access to information about how
 335 the final user message, for example, attends to the rest of the context. Our method is therefore
 336 benchmarked against baselines that have access to more direct, query-specific information at the time
 337 of compression. We highlight in all the figures the attention-based baselines with dashed lines.

338
 339 **Absolute vs. Relative Cache Size.** A final methodological note concerns our use of cache size.
 340 Throughout our evaluation, we report performance as a function of absolute KV cache size (i.e.,
 341 the number of tokens retained) rather than a relative compression ratio. This decision is motivated
 342 by practical application: practitioners operate under fixed memory constraints, making an absolute
 343 token budget a more direct and interpretable measure of resource cost. In contrast, a compression
 344 ratio’s impact on memory is dependent on the initial context length, making it a less stable metric for
 345 cross-scenario comparison.

346 4.2 DOWNSTREAM PERFORMANCE

347 This section assesses the real-world efficacy of each compression method. We apply the strategies to
 348 a live LLM, reducing the KV cache to a target budget after the prefill before measuring performance
 349 on several downstream benchmarks.



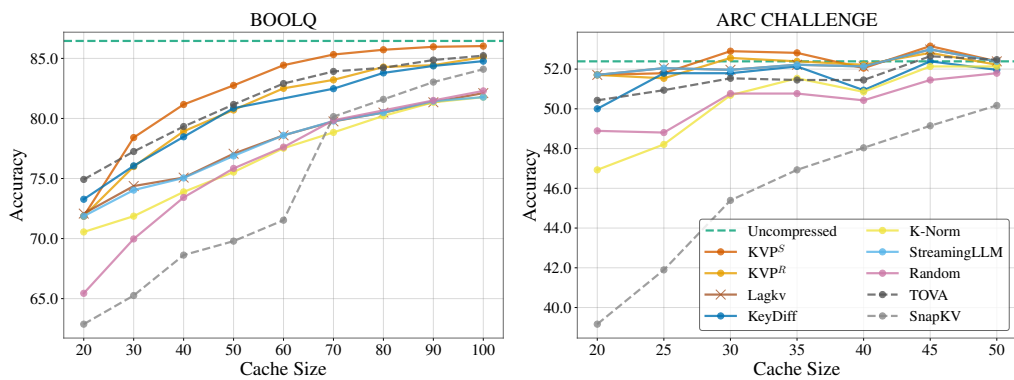
364 Figure 2: Overall accuracy on the RULER benchmark (Left) and perplexity on the OASST2-4k test
 365 set (Right), as a function of the absolute KV cache size. KVP achieves the highest accuracy and
 366 lowest perplexity across most of the possible cache sizes.

367
 368 **RULER benchmark.** We evaluate performance on the RULER benchmark using its official text-
 369 based accuracy metric, which requires generating the correct answer for long-context reasoning tasks.
 370 This tests whether the methods preserve the specific, often non-local, information needed for complex
 371 problem-solving. Figure 2 (left) shows that KVP consistently outperforms all baselines, retaining
 372 higher accuracy as the cache budget shrinks. This result is a direct consequence of its learned policy:
 373 unlike heuristics that might discard old but crucial clues, KVP learns to identify and keep these
 374 high-value tokens, regardless of their position, enabling the model to succeed at the task. A detailed
 375 breakdown of performance across all RULER subtasks, along with their corresponding eviction error
 376 curves, is provided in Figure 12, further highlighting the robustness of our method. This result is
 377 particularly noteworthy given that RULER’s structure heavily favors strategies that can use the final
 378 question to identify relevant context; an advantage held by attention-based baselines but not by KVP.

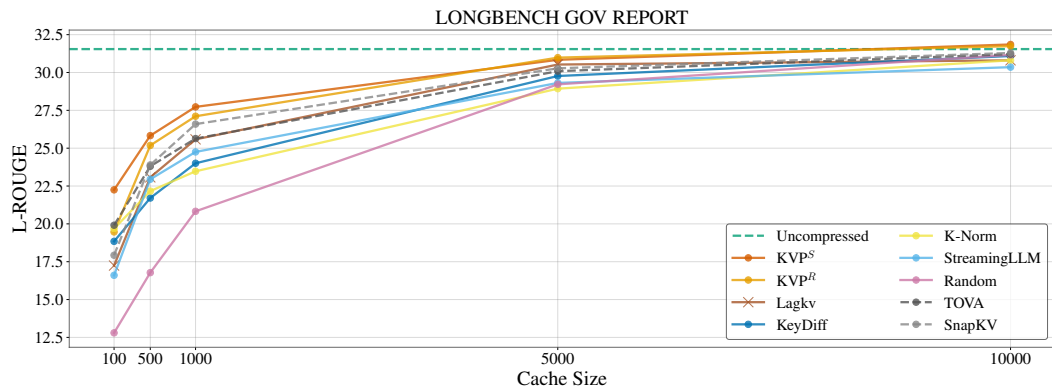
378 **OASST2 benchmark.** We evaluate the efficacy of KV cache compression by its impact on perplexity (PPL), a measure of the model’s next-token prediction capability. An effective compression
 379 method should minimize PPL degradation. As shown in Figure 2 (right), KVP consistently achieves
 380 lower perplexity than baselines that rely solely on KV embeddings. Furthermore, it often outperforms
 381 methods that use additional information across nearly all cache sizes. In contrast, heuristic approaches
 382 like *StreamingLLM* exhibit a sharp increase in PPL as the cache budget decreases, confirming the
 383 brittleness of their fixed-rule strategies. The superior performance of KVP demonstrates a direct link
 384 between our training objective and the preservation of the model’s downstream capabilities. These
 385 findings are further corroborated by results on the RULER benchmark (Appendix Figure 9), where
 386 KVP maintains a similar advantage.
 387

388
 389 **Generalization to other benchmarks.** LLMs are widely regarded as general-purpose computational
 390 systems and their utility depends on robust performance in out-of-domain scenarios. Even
 391 though KVP enables efficient training of domain specific policy using only unlabelled dataset of se-
 392 quences, we evaluate its zero-shot generalization performance on a set of standard downstream tasks.
 393 Specifically, we test agents trained on RULER (KVP^R) and *OASST2* (KVP^S) on *ARC-Challenge*,
 394 *BoolQ*, and the *GovReport* task from the LongBench benchmark, reporting performance at vary-
 395 ing KV cache sizes. Importantly, the “prefill” stage does not include the question in *BoolQ* and
 396 *GovReport*, so as to better reflect real-world scenarios where a given text is compressed for differ-
 397 ent questions not known in advance. Results on *MMLU* and *HellaSwag* are instead presented in
 398 Appendix A.4. This evaluation is designed to assess whether policies optimized for long-context
 399 efficiency maintain performance on short and long-context benchmarks that probe factual knowledge,
 400 multi-step reasoning, and commonsense inference.
 401

402 The results, presented in Figures 3 and 4, demonstrate that KVP consistently achieves competitive
 403 performance. Across the diverse benchmarks, both KVP^R and KVP^S rank at or near the top,
 404 outperforming most heuristic baselines and closely tracking the accuracy of the uncompressed model,
 405 demonstrating minimal degradation at different cache size reduction. While both agents generalize
 406 effectively, some specialization emerges: KVP^S (trained on conversational data) shows an advantage
 407 on the natural question answering task *BoolQ* and the summarization task *GovReport*, whereas
 408 KVP^R (trained on synthetic reasoning sequences) performs best on the expert-knowledge benchmark
 409 *MMLU* as shown in Figure 10 in Appendix A.4. In contrast to the baselines, whose relative ranking
 410 is inconsistent across benchmarks, these results highlight that the adaptive policy learned by KVP
 411 generalizes far beyond their training domain and context lengths. This success preserves the model’s
 412 core capabilities, confirming that KVP is not a specialized tool with significant trade-offs, but a robust
 413 technique that can be enabled by default to provide memory savings while minimizing degradation to
 414 the model’s general utility.
 415



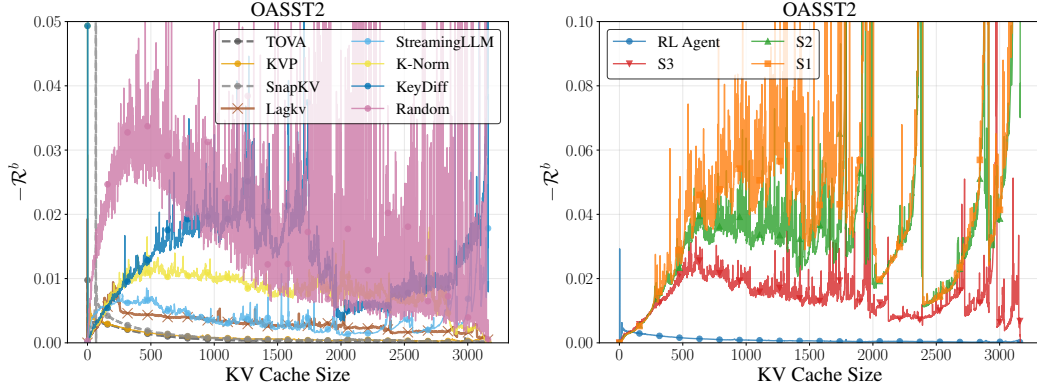
416
 417 Figure 3: Average test accuracy on (Left) BoolQ and (Right) ARC Challenge as a function of KV
 418 cache size. Higher is better.
 419
 420
 421
 422
 423
 424
 425
 426
 427
 428
 429
 430
 431



445 Figure 4: Average test L-Rouge score on the GovReport as a function of KV cache size. Higher is
446 better.
447
448

449 4.3 ABLATIONS

450 To validate the core design choices of KVP, we conduct two key ablation studies. First, we analyze
451 our proposed reward function, as defined in Equation (4). Second, we study our use of RL instead of
452 supervised surrogates of sorting.
453



467 (a) **Effectiveness of the reward:** KVP performs on par
468 with attention-aware methods (dashed lines) despite
469 not using their privileged information by learning to
470 predict future attentions. A full visualization for all the
471 layers is in Figures 13 and 14.

467 (b) **RL vs Supervised Surrogates of Sorting:** The RL
468 agent successfully reaches low cost ($-\mathcal{R}^b$) while the
469 supervised surrogate (Blondel et al., 2020) fails. We
470 tested the supervised approach with three learning rates:
471 5×10^{-6} , 5×10^{-5} and 5×10^{-4} .

471 Figure 5: Cost per-budget ($-\mathcal{R}^b$) on the OASST2 test set for a representative head (layer 10, head 0).
472
473

474 **Is the reward function \mathcal{R} effective?** To confirm that our reward \mathcal{R} enables effective learning of
475 eviction policies, we measure the negative per-budget reward, $-\mathcal{R}^b$, on unseen test data. This value
476 corresponds to the total future importance of the tokens evicted at a given budget b which our agent is
477 trained to minimize across all budgets simultaneously.

478 The results in Figure 5a show a clear separation between methods: while attention-aware methods
479 that use query information at inference time (dashed lines) form a distinct, low-loss cluster, heuristics
480 without attention scores form a high-loss cluster. This is rather expected as the target, future attention
481 scores, is highly related to attention. Crucially, KVP performs within this top-tier group, achieving
482 a loss comparable to methods like *TOVA* and *SnapKV* without using their privileged information.
483 This demonstrates that our offline RL training successfully distills the principles of attention-based
484 ranking into an efficient, static policy. Furthermore, the analysis reveals the importance of policy
485 specialization across heads. A fixed heuristic like *StreamingLLM* can be effective for certain heads
(see layer 22, head 0 in Figure 14) but detrimental for others (see layer 19, head 0 in Figure 13). Even

486 *KeyDiff*, a strong attention-free heuristic, exhibits hard failure modes (see layer 2, head 0 in Figure 14).
 487 This result, together with a comprehensive sweeps across all layers and heads in Figures 13 and 14,
 488 confirms that KVP learns diverse patterns that cannot be captured with a single heuristic.
 489

490 **Is RL necessary?** We ablate the necessity of using RL by comparing it to a supervised learning
 491 baseline using differentiable surrogate of sorting (Blondel et al., 2020). This baseline uses the same
 492 data and network architecture but replaces the policy gradient objective with a length-normalized
 493 Mean Squared Error loss between predicted soft ranks (from a differentiable sorter (Blondel et al.,
 494 2020)) and the ground-truth ranks. As shown in Figure 5b, this leads to poor performance: the
 495 supervised agent fails to learn an effective policy, evidenced by its high and unstable cost curve. In
 496 contrast, the RL agent’s cost is low and stable confirming that RL is better suited for learning KV
 497 cache policies.

498 We conjecture that the KV cache eviction task is inherently sparse: only a small fraction of tokens are
 499 critical for future generation. This sparsity poses a fundamental challenge for supervised methods
 500 using differentiable sorting surrogates. Such methods face a trade-off: a low temperature provides
 501 vanishing gradients, while a high temperature yields dense but biased gradients that incorrectly
 502 disperse importance across irrelevant tokens. Policy gradient methods bypass this issue by providing
 503 an unbiased learning signal through the non-differentiable sort operation. This allows for direct credit
 504 assignment, concentrating the learning signal on the few ranking decisions that matter.

506 5 CONCLUSIONS AND FUTURE WORK

507 In this work, we introduced a new paradigm for KV cache eviction by reframing it as a learnable
 508 sorting problem. We proposed KVP, a system of lightweight, per-head policies trained to rank cache
 509 entries by their predicted future utility. The core of our method is a reward signal based on the
 510 ranking quality across all possible memory budgets and its efficient inference-free optimization via
 511 reinforcement learning. This approach allows for fine-grained, adaptive memory control without
 512 requiring architectural changes or costly live LLM inference during training.

513 Our evaluations on long-context benchmarks demonstrate that KVP consistently outperforms strong
 514 heuristic baselines, achieving lower perplexity degradation and higher task accuracy under tight
 515 memory constraints. This validates our central hypothesis: directly learning a specialized sorting
 516 policy is a more powerful and robust strategy than relying on handcrafted, backward-looking proxies
 517 for token importance. By preserving model fidelity more effectively, KVP establishes a promising
 518 direction for building more efficient and capable LLM inference systems.

519 Future work could extend this framework in several exciting directions. A natural next step is to
 520 develop an adaptive budget allocation policy that dynamically assigns memory where it is most
 521 needed across heads and layers. Furthermore, while KVP is highly efficient, it does not model inter-
 522 dependencies between heads. A powerful extension would be to explore joint, end-to-end optimization
 523 of all policies, which could capture these complex dynamics at the cost of requiring online training.

524 REFERENCES

525 Marah Abdin, Sahaj Agarwal, Ahmed Awadallah, Vidhisha Balachandran, Harkirat Behl, Lingjiao
 526 Chen, Gustavo de Rosa, Suriya Gunasekar, Mojan Javaheripi, Neel Joshi, Piero Kauffmann, Yash
 527 Lara, Caio César Teodoro Mendes, Arindam Mitra, Besmira Nushi, Dimitris Papailiopoulos,
 528 Olli Saarikivi, Shital Shah, Vaishnavi Shrivastava, Vibhav Vineet, Yue Wu, Safoora Yousefi, and
 529 Guoqing Zheng. Phi-4-reasoning technical report, 2025. URL <https://arxiv.org/abs/2504.21318>.

530 Muhammad Adnan, Akhil Arunkumar, Gaurav Jain, Prashant J. Nair, Ilya Soloveychik,
 531 and Purushotham Kamath. Keyformer: Kv cache reduction through key tokens se-
 532 lection for efficient generative inference. In P. Gibbons, G. Pekhimenko, and C. De
 533 Sa (eds.), *Proceedings of Machine Learning and Systems*, volume 6, pp. 114–127,
 534 2024. URL https://proceedings.mlsys.org/paper_files/paper/2024/file/48fecef47b19fe501d27d338b6d52582-Paper-Conference.pdf.

540 Sadia Afrin, Md Abdullah All Mahmud, Abdus Salam, Md Abdullah Al Jubair, and Muhammad Firoz
 541 Mridha. Machine learning for predictive database caching strategies: A state-of-the-art review. In
 542 *Proceedings of the 3rd International Conference on Computing Advancements*, ICCA 2024, pp.
 543 540–547. ACM, 2024. doi: 10.1145/3723178.3723250.

544 Arash Ahmadian, Chris Cremer, Matthias Gallé, Marzieh Fadaee, Julia Kreutzer, Olivier Pietquin,
 545 Ahmet Üstün, and Sara Hooker. Back to basics: Revisiting reinforce style optimization for
 546 learning from human feedback in llms. *ArXiv preprint*, abs/2402.14740, 2024. URL <https://arxiv.org/abs/2402.14740>.

547 Joshua Ainslie, James Lee-Thorp, Michiel de Jong, Yury Zemlyanskiy, Federico Lebron, and Sumit
 548 Sanghai. GQA: Training generalized multi-query transformer models from multi-head checkpoints.
 549 In *EMNLP*, Singapore, 2023.

550 Anonymous. Icecache: Memory-efficient KV-cache management for long-sequence LLMs. In
 551 *Submitted to The Fourteenth International Conference on Learning Representations*, 2025. URL
 552 <https://openreview.net/forum?id=yHxSKM9kdr>. under review.

553 Yushi Bai, Xin Lv, Jiajie Zhang, Hong Lyu, Jiankai Tang, Zhidean Huang, Zhengxiao Du, Xiao
 554 Liu, Aohan Zeng, Lei Hou, Yuxiao Dong, Jie Tang, and Juanzi Li. Longbench: A bilingual,
 555 multitask benchmark for long context understanding. *ArXiv*, abs/2308.14508, 2023. URL <https://api.semanticscholar.org/CorpusID:261245264>.

556 Mathieu Blondel, Olivier Teboul, Quentin Berthet, and Josip Djolonga. Fast differentiable sorting
 557 and ranking. In *ICML*, 2020.

558 Tom B. Brown, Benjamin Mann, Nick Ryder, Melanie Subbiah, Jared Kaplan, Prafulla Dhariwal,
 559 Arvind Neelakantan, Pranav Shyam, Girish Sastry, Amanda Askell, Sandhini Agarwal, Ariel
 560 Herbert-Voss, Gretchen Krueger, Tom Henighan, Rewon Child, Aditya Ramesh, Daniel M. Ziegler,
 561 Jeffrey Wu, Clemens Winter, Christopher Hesse, Mark Chen, Eric Sigler, Mateusz Litwin, Scott
 562 Gray, Benjamin Chess, Jack Clark, Christopher Berner, Sam McCandlish, Alec Radford, Ilya
 563 Sutskever, and Dario Amodei. Language models are few-shot learners. In *NeurIPS*, 2020.

564 Zefan Cai, Yichi Zhang, Bofei Gao, Yuliang Liu, Tianyu Liu, Keming Lu, Wayne Xiong, Yue
 565 Dong, Baobao Chang, Junjie Hu, and Wen Xiao. Pyramidkv: Dynamic kv cache compression
 566 based on pyramidal information funneling. *ArXiv preprint*, abs/2406.02069, 2024. URL <https://arxiv.org/abs/2406.02069>.

567 Edoardo Cetin, Qi Sun, Tianyu Zhao, and Yujin Tang. An evolved universal transformer memory.
 568 *ArXiv preprint*, abs/2410.13166, 2024. URL <https://arxiv.org/abs/2410.13166>.

569 Vivek Chari, Guanghui Qin, and Benjamin Van Durme. Kv-distill: Nearly lossless learnable context
 570 compression for llms. *ArXiv preprint*, abs/2503.10337, 2025. URL <https://arxiv.org/abs/2503.10337>.

571 Renze Chen, Zhuofeng Wang, Beiquan Cao, Tong Wu, Size Zheng, XiuHong Li, XueChao Wei,
 572 Shengen Yan, Meng Li, and Yun Liang. Arkvale: Efficient generative LLM inference with
 573 recallable key-value eviction. In *The Thirty-eighth Annual Conference on Neural Information
 574 Processing Systems*, 2024a. URL <https://openreview.net/forum?id=4oAt5L41Ye>.

575 Shaoyuan Chen, Yutong Lin, Mingxing Zhang, and Yongwei Wu. Efficient and economic large
 576 language model inference with attention offloading. *ArXiv preprint*, abs/2405.01814, 2024b. URL
 577 <https://arxiv.org/abs/2405.01814>.

578 Zhuoming Chen, Ranajoy Sadhukhan, Zihao Ye, Yang Zhou, Jianyu Zhang, Niklas Nolte, Yuandong
 579 Tian, Matthijs Douze, Leon Bottou, Zihao Jia, and Beidi Chen. MagicPIG: LSH sampling for
 580 efficient LLM generation. In *The Thirteenth International Conference on Learning Representations*,
 581 2025. URL <https://openreview.net/forum?id=ALzTQUGW8a>.

582 Christopher Clark, Kenton Lee, Ming-Wei Chang, Tom Kwiatkowski, Michael Collins, and Kristina
 583 Toutanova. Boolq: Exploring the surprising difficulty of natural yes/no questions. In *NAACL*,
 584 2019.

594 Peter Clark, Isaac Cowhey, Oren Etzioni, Tushar Khot, Ashish Sabharwal, Carissa Schoenick, and
 595 Oyvind Tafjord. Think you have solved question answering? try arc, the ai2 reasoning challenge.
 596 *arXiv:1803.05457v1*, 2018.

597

598 Tri Dao, Daniel Y Fu, Stefano Ermon, Atri Rudra, and Christopher Re. Flashattention: Fast and
 599 memory-efficient exact attention with IO-awareness. In Alice H. Oh, Alekh Agarwal, Danielle
 600 Belgrave, and Kyunghyun Cho (eds.), *Advances in Neural Information Processing Systems*, 2022.
 601 URL <https://openreview.net/forum?id=H4DqfPSibmx>.

602 Chenlong Deng, Zhisong Zhang, Kelong Mao, Shuaiyi Li, Tianqing Fang, Hongming Zhang, Haitao
 603 Mi, Dong Yu, and Zhicheng Dou. Unigist: Towards general and hardware-aligned sequence-
 604 level long context compression. In *The Thirty-ninth Annual Conference on Neural Information
 605 Processing Systems*, 2025. URL <https://openreview.net/forum?id=1C4mXyh31p>.

606

607 Tim Dettmers, Mike Lewis, Younes Belkada, and Luke Zettlemoyer. Llm.int8(): 8-bit matrix
 608 multiplication for transformers at scale. *ArXiv preprint*, abs/2208.07339, 2022. URL <https://arxiv.org/abs/2208.07339>.

609

610 Alessio Devoto, Yu Zhao, Simone Scardapane, and Pasquale Minervini. A simple and effective
 611 l_2 norm-based strategy for kv cache compression. *ArXiv preprint*, abs/2406.11430, 2024. URL
 612 <https://arxiv.org/abs/2406.11430>.

613

614 Leo Gao, Jonathan Tow, Baber Abbasi, Stella Biderman, Sid Black, Anthony DiPofi, Charles Foster,
 615 Laurence Golding, Jeffrey Hsu, Alain Le Noac'h, Haonan Li, Kyle McDonell, Niklas Muennighoff,
 616 Chris Ociepa, Jason Phang, Laria Reynolds, Hailey Schoelkopf, Aviya Skowron, Lintang Sutawika,
 617 Eric Tang, Anish Thite, Ben Wang, Kevin Wang, and Andy Zou. The language model evaluation
 618 harness, 2024. URL <https://zenodo.org/records/12608602>.

619

620 Suyu Ge, Yunan Zhang, Liyuan Liu, Minjia Zhang, Jiawei Han, and Jianfeng Gao. Model tells you
 621 what to discard: Adaptive KV cache compression for llms. In *ICLR*, 2024.

622

623 Ravi Ghadia, Avinash Kumar, Gaurav Jain, Prashant J. Nair, and Poulami Das. Dialogue without
 624 limits: Constant-sized KV caches for extended response in LLMs. In *Forty-second International
 625 Conference on Machine Learning*, 2025. URL <https://openreview.net/forum?id=SuYO70ZxZX>.

626

627 Aditya Grover, Eric Wang, Aaron Zweig, and Stefano Ermon. Stochastic optimization of sorting
 628 networks via continuous relaxations. In *ICLR*, 2019.

629

630 Dan Hendrycks, Collin Burns, Steven Basart, Andy Zou, Mantas Mazeika, Dawn Song, and Jacob
 631 Steinhardt. Measuring massive multitask language understanding. In *ICLR*, 2021.

632

633 Cheng-Ping Hsieh, Simeng Sun, Samuel Kriman, Shantanu Acharya, Dima Rekesh, Fei Jia, Yang
 634 Zhang, and Boris Ginsburg. Ruler: What's the real context size of your long-context language
 635 models? *ArXiv preprint*, abs/2404.06654, 2024. URL <https://arxiv.org/abs/2404.06654>.

636

637 Andreas Köpf, Yannic Kilcher, Dimitri von Rütte, Sotiris Anagnostidis, Zhi Rui Tam, Keith Stevens,
 638 Abdullah Barhoum, Duc Nguyen, Oliver Stanley, Richárd Nagyfi, Shahul ES, Sameer Suri, David
 639 Glushkov, Arnav Dantuluri, Andrew Maguire, Christoph Schuhmann, Huu Nguyen, and Alexander
 640 Mattick. Openassistant conversations - democratizing large language model alignment. In *NeurIPS*,
 2023.

641

642 Wonbeom Lee, Jungi Lee, Junghwan Seo, and Jaewoong Sim. Infinigen: Efficient generative inference
 643 of large language models with dynamic kv cache management. *ArXiv preprint*, abs/2406.19707,
 644 2024a. URL <https://arxiv.org/abs/2406.19707>.

645

646 Wonbeom Lee, Jungi Lee, Junghwan Seo, and Jaewoong Sim. Infinigen: efficient generative inference
 647 of large language models with dynamic kv cache management. In *Proceedings of the 18th USENIX
 648 Conference on Operating Systems Design and Implementation*, OSDI'24, USA, 2024b. USENIX
 Association. ISBN 978-1-939133-40-3.

648 Yuhong Li, Yingbing Huang, Bowen Yang, Bharat Venkitesh, Acyr Locatelli, Hanchen Ye, Tianle
 649 Cai, Patrick Lewis, and Deming Chen. Snapkv: LLM knows what you are looking for before
 650 generation. In *NeurIPS*, 2024.

651

652 Manlai Liang, JiaMing Zhang, Xiong Li, and Jinlong Li. Lagkv: Lag-relative information of the kv
 653 cache tells which tokens are important. *ArXiv*, abs/2504.04704, 2025.

654 Gonzalo Mena, David Belanger, Scott Linderman, and Jasper Snoek. Learning latent permutations
 655 with gumbel-sinkhorn networks. In *ICLR*, 2018.

656

657 Piotr Nawrot, Adrian Lancucki, Marcin Chochowski, David Tarjan, and Edoardo M. Ponti. Dynamic
 658 memory compression: Retrofitting llms for accelerated inference. In *ICML*, 2024.

659 G. L. Nemhauser, L. A. Wolsey, and M. L. Fisher. An analysis of approximations for maximizing
 660 submodular set functions. *Mathematical Programming*, 14(1):265–294, 1978.

661

662 Abdullah Önden and Mohammed Alnour. Chatgpt and openai: A comprehensive bibliometric review.
 663 *Journal of Soft Computing and Decision Analytics*, 1(1):254–264, 2023.

664 Matanel Oren, Michael Hassid, Nir Yarden, Yossi Adi, and Roy Schwartz. Transformers are multi-
 665 state rnns. *ArXiv preprint*, abs/2401.06104, 2024. URL <https://arxiv.org/abs/2401.06104>.

666

667 Junyoung Park, Dalton Jones, Matthew J Morse, Raghav Goel, Mingu Lee, and Chris Lott. Keydiff:
 668 Key similarity-based kv cache eviction for long-context llm inference in resource-constrained
 669 environments. *ArXiv preprint*, abs/2504.15364, 2025. URL <https://arxiv.org/abs/2504.15364>.

670

671

672 R. L. Plackett. The analysis of permutations. *Journal of the Royal Statistical Society*, 24(2):193–202,
 673 1975.

674

675 Sebastian Prillo and Julian Martin Eisenschlos. Softsort: A continuous relaxation for the argsort
 676 operator. In *ICML*, 2020.

677

678 Luka Ribar, Ivan Chelombiev, Luke Hudlass-Galley, Charlie Blake, Carlo Luschi, and Douglas Orr.
 Sparq attention: Bandwidth-efficient LLM inference. In *ICML*, 2024.

679

680 Ying Sheng, Lianmin Zheng, Binhang Yuan, Zuhuan Li, Max Ryabinin, Beidi Chen, Percy Liang,
 681 Christopher Ré, Ion Stoica, and Ce Zhang. Flexgen: High-throughput generative inference of large
 682 language models with a single GPU. In *ICML*, 2023.

683

Junaid Shuja, Kashif Bilal, Waleed Alasmary, Hassan Sinky, and Eisa Alanazi. Applying machine
 684 learning techniques for caching in edge networks: A comprehensive survey. *ArXiv preprint*,
 685 abs/2006.16864, 2020. URL <https://arxiv.org/abs/2006.16864>.

686

Prajwal Singhania, Siddharth Singh, Shwai He, Soheil Feizi, and Abhinav Bhatele. Loki: Low-rank
 687 keys for efficient sparse attention. In *NeurIPS*, 2024.

688

Jiaming Tang, Yilong Zhao, Kan Zhu, Guangxuan Xiao, Baris Kasikci, and Song Han. QUEST:
 689 query-aware sparsity for efficient long-context LLM inference. In *ICML*, 2024.

690

Hugo Touvron, Louis Martin, Kevin Stone, Peter Albert, Amjad Almahairi, Yasmine Babaei, Nikolay
 691 Bashlykov, Soumya Batra, Prajjwal Bhargava, Shruti Bhosale, et al. Llama 2: Open foundation
 692 and fine-tuned chat models. *ArXiv preprint*, abs/2307.09288, 2023. URL <https://arxiv.org/abs/2307.09288>.

693

Ashish Vaswani, Noam Shazeer, Niki Parmar, Jakob Uszkoreit, Llion Jones, Aidan N. Gomez, Lukasz
 694 Kaiser, and Illia Polosukhin. Attention is all you need. In *NIPS*, 2017.

695

Peng Wang, Shuai Bai, Sinan Tan, Shijie Wang, Zhihao Fan, Jinze Bai, Keqin Chen, Xuejing
 696 Liu, Jialin Wang, Wenbin Ge, Yang Fan, Kai Dang, Mengfei Du, Xuancheng Ren, Rui Men,
 697 Dayiheng Liu, Chang Zhou, Jingren Zhou, and Junyang Lin. Qwen2-vl: Enhancing vision-
 698 language model’s perception of the world at any resolution. *ArXiv preprint*, abs/2409.12191, 2024.
 699 URL <https://arxiv.org/abs/2409.12191>.

702 Yantong Wang and Vasilis Friderikos. A survey of deep learning for data caching in edge network.
 703 *ArXiv preprint*, abs/2008.07235, 2020. URL <https://arxiv.org/abs/2008.07235>.

704 Ronald J. Williams. Simple statistical gradient-following algorithms for connectionist reinforcement
 705 learning. *Machine Learning*, 8(3–4):229–256, 1992.

706 Guangxuan Xiao, Ji Lin, Mickaël Seznec, Hao Wu, Julien Demouth, and Song Han. Smoothquant:
 707 Accurate and efficient post-training quantization for large language models. In *ICML*, 2023.

708 Guangxuan Xiao, Yuandong Tian, Beidi Chen, Song Han, and Mike Lewis. Efficient streaming
 709 language models with attention sinks. In *ICLR*, 2024.

710 An Yang, Baosong Yang, Binyuan Hui, Bo Zheng, Bowen Yu, Chang Zhou, Chengpeng Li,
 711 Chengyuan Li, Dayiheng Liu, Fei Huang, Guanting Dong, Haoran Wei, Huan Lin, Jialong Tang,
 712 Jialin Wang, Jian Yang, Jianhong Tu, Jianwei Zhang, Jianxin Ma, Jianxin Yang, Jin Xu, Jingren
 713 Zhou, Jinze Bai, Jinzheng He, Junyang Lin, Kai Dang, Keming Lu, Keqin Chen, Kexin Yang,
 714 Mei Li, Mingfeng Xue, Na Ni, Pei Zhang, Peng Wang, Ru Peng, Rui Men, Ruize Gao, Runji Lin,
 715 Shijie Wang, Shuai Bai, Sinan Tan, Tianhang Zhu, Tianhao Li, Tianyu Liu, Wenbin Ge, Xiaodong
 716 Deng, Xiaohuan Zhou, Xingzhang Ren, Xinyu Zhang, Xipin Wei, Xuancheng Ren, Xuejing Liu,
 717 Yang Fan, Yang Yao, Yichang Zhang, Yu Wan, Yunfei Chu, Yuqiong Liu, Zeyu Cui, Zhenru Zhang,
 718 Zhipang Guo, and Zhihao Fan. Qwen2 technical report. *ArXiv preprint*, abs/2407.10671, 2024.
 719 URL <https://arxiv.org/abs/2407.10671>.

720 Rowan Zellers, Ari Holtzman, Yonatan Bisk, Ali Farhadi, and Yejin Choi. Hellaswag: Can a machine
 721 really finish your sentence? In *ACL*, 2019.

722 Peitian Zhang, Zheng Liu, Shitao Xiao, Ninglu Shao, Qiwei Ye, and Zhicheng Dou. Long context
 723 compression with activation beacon. In *The Thirteenth International Conference on Learning
 724 Representations*, 2025. URL <https://openreview.net/forum?id=1eQT9OzfNQ>.

725 Zhenyu Zhang, Ying Sheng, Tianyi Zhou, Tianlong Chen, Lianmin Zheng, Ruisi Cai, Zhao Song,
 726 Yuandong Tian, Christopher Ré, Clark W. Barrett, Zhangyang Wang, and Beidi Chen. H2O:
 727 heavy-hitter oracle for efficient generative inference of large language models. In *NeurIPS*, 2023.

731 A APPENDIX

732 A.1 MISSING PROOF OF PROPOSITION 1

733 *Proof.* Since $|S_{b+1}^*| = b+1$ and $|S_b^*| = b$ with $S_b^* \subset S_{b+1}^*$, the set difference $S_{b+1}^* \setminus S_b^*$ is nonempty.
 734 By uniqueness of S_{b+1}^* , this difference must contain exactly one element; otherwise, there would
 735 exist two distinct $(b+1)$ -subsets strictly between S_b^* and S_{b+1}^* , contradicting uniqueness. Hence we
 736 can define a sequence of distinct elements

$$737 x_{\sigma_1} \in S_1^*, \quad x_{\sigma_{b+1}} \in S_{b+1}^* \setminus S_b^* \quad (b = 1, \dots, n-1).$$

738 By construction, for each b we have

$$739 S_b^* = \{x_{\sigma_1}, \dots, x_{\sigma_b}\}.$$

740 Now define a total order (ranking) π on $[n]$ by setting

$$741 \pi(x_{\sigma_b}) = b \quad (b = 1, \dots, n).$$

742 This is a bijection $\pi : [n] \rightarrow [n]$, and its top- b prefix is precisely $\{x_{\sigma_1}, \dots, x_{\sigma_b}\} = S_b^*$. Therefore,

$$743 S_b^* = \{i \in [n] : \pi(i) \leq b\} \quad \text{for all } b,$$

744 as claimed.

745 Equivalently, given π we may define a scoring function consistent with the order, for instance

$$746 s(x_{\sigma_k}) = n - k \quad (k = 1, \dots, n),$$

747 which is strictly decreasing in k . Then the top- b elements according to s are exactly
 748 $\{x_{\sigma_1}, \dots, x_{\sigma_b}\} = S_b^*$. \square

756
757

A.2 IMPLEMENTATION DETAILS

758
759
760
761
762

Our KVP agents are lightweight 2-layer MLPs with 256 hidden units, trained using the RLOO algorithm (Ahmadian et al., 2024) as described in Section 3. Following the Grouped-Query Attention (GQA) architecture of Qwen2.5-7B-Chat, we train a separate agent for each of the 4 KV heads across all 28 layers, yielding 112 specialized agents. Each agent contains approximately 600K parameters.

763
764
765
766
767

The agents are optimized to maximize the reward signal in Equation (4), which encourages retention of tokens with high future utility across all cache budgets. During inference, the learned policy ranks all tokens except the first 4 and last 16, which are always retained. Token eviction is emulated via custom attention masks in FlexAttention, preventing the model from attending to pruned tokens during generation.

768
769
770
771
772

For training stability, we apply gradient clipping (maximum norm of 5) and normalize advantages by their mean and standard deviation, without entropy regularization. We use AdamW with a learning rate of 5×10^{-5} , following a cosine schedule with 100-step linear warmup (start factor 0.01) that decays to 1×10^{-6} . Each agent trains for 4,000 steps on pre-computed activations.

773
774

A.3 TRAINING AND MEMORY OVERHEAD

775
776
777
778
779
780
781
782
783

The training process for our KVP agents is designed to be highly efficient, imposing minimal computational and storage overhead. Agents are trained on a small dataset of pre-computed activation traces; for our experiments, we used approximately 6,000 samples from the RULER dataset and 4,500 from the OASST2 dataset. Data generation represents the primary one-time cost of this pipeline, requiring a single forward pass over these training samples to collect and store on disk the Query, Key, and Value embeddings for the entire generation sequence for each KV cache. This step incurs a computational cost approximately equivalent to standard inference on the dataset. Each per-head agent is a small MLP with approximately 650K parameters, resulting in a checkpoint size of only 2.6MB.

784
785
786
787
788
789

The agent training completes in less than 30 minutes on a single node of 8 NVIDIA H100 GPUs. We note that this training time is achieved without extensive hyperparameter tuning or code optimizations for speed, suggesting that further significant speed-ups are possible. These factors highlight the low computational footprint of our offline training framework.

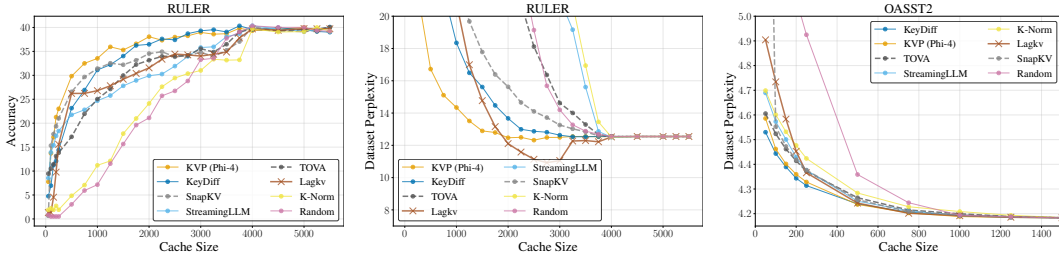
790
791
792
793
794
795
796
797
798
799
800
801

FLOPs estimation. To assess computational cost independent of hardware optimization (e.g., kernel fusion), we quantify the FLOPs overhead per token:

- Autoregressive Generation (Throughput). Zero Overhead. In our setting, the KV cache is compressed only once after prefill. This means KVP introduces no additional FLOPs during the decoding phase. Consequently, its throughput is identical to any other eviction method at the same cache budget. KVP’s contribution is achieving superior accuracy for that given level of throughput.
- Prefill Latency. Cost: 14.00 GFLOPs \rightarrow 14.15 GFLOPs. The overhead is strictly confined to the prefill stage. Based on the standard approximation of $2 \times N_{params}$ FLOPs per token:
 - Base model (Qwen-7B): 14.00 GFLOPs/token.
 - KVP Overhead: Our 112 agents (0.65M params each) add 72.8M parameters, contributing an additional 0.15 GFLOPs/token.
 - Total: The prefill cost becomes 14.15 GFLOPs/token, a marginal increase of 1%.

802
803
804
805
806
807
808
809

This quantitative breakdown demonstrates that the computational footprint of KVP is negligible compared to the backbone model.

810 A.4 ADDITIONAL RESULTS
811

812
813
814
815
816
817
818
819
820
821
822
823
824
825
826
827
828
829
830
831
832
833
834
835
836
837
838
839
840
841
842
843
844
845
846
847
848
849
850
851
852
853
854
855
856
857
858
859
860
861
862
863

Figure 6: Evaluation of our KVP eviction strategy on the Phi-4 14B model. The results demonstrate that our learning framework generalizes effectively to a different model architecture. While KVP’s performance remains consistently strong, the relative performance of heuristic baselines changes significantly between Qwen 2.5 and Phi-4. This provides strong evidence that their effectiveness is model-dependent, unlike our learned approach. **(left)** KVP achieves the high accuracy on the RULER benchmark, successfully adapting its learned policy where attention-based heuristics (SnapKV, TOVA) fail due to the task’s nature. **(center)** Perplexity on the RULER test set, where KVP consistently outperforms baselines. **(right)** Perplexity on the OASST2-4k test set, confirming KVP’s good performance.

Future Attention Importance

I’m planning a trip to Rome next month. I want to visit the Colosseum, the Vatican Museums, and the Trevi Fountain. What’s the best order to visit these attractions to minimize travel time? <|im_end|> Also, should I book tickets in advance for these places? <|im_end|>

KVP

I’m planning a trip to Rome next month. I want to visit the Colosseum, the Vatican Museums, and the Trevi Fountain. What’s the best order to visit these attractions to minimize travel time? <|im_end|> Also, should I book tickets in advance for these places? <|im_end|>

SnapKV

I’m planning a trip to Rome next month. I want to visit the Colosseum, the Vatican Museums, and the Trevi Fountain. What’s the best order to visit these attractions to minimize travel time? <|im_end|> Also, should I book tickets in advance for these places? <|im_end|>

KeyDiff

I’m planning a trip to Rome next month. I want to visit the Colosseum, the Vatican Museums, and the Trevi Fountain. What’s the best order to visit these attractions to minimize travel time? <|im_end|> Also, should I book tickets in advance for these places? <|im_end|>

LagKV

I’m planning a trip to Rome next month. I want to visit the Colosseum, the Vatican Museums, and the Trevi Fountain. What’s the best order to visit these attractions to minimize travel time? <|im_end|> Also, should I book tickets in advance for these places? <|im_end|>

StreamingLLM

I’m planning a trip to Rome next month. I want to visit the Colosseum, the Vatican Museums, and the Trevi Fountain. What’s the best order to visit these attractions to minimize travel time? <|im_end|> Also, should I book tickets in advance for these places? <|im_end|>

KNorm

I’m planning a trip to Rome next month. I want to visit the Colosseum, the Vatican Museums, and the Trevi Fountain. What’s the best order to visit these attractions to minimize travel time? <|im_end|> Also, should I book tickets in advance for these places? <|im_end|>

Random

I’m planning a trip to Rome next month. I want to visit the Colosseum, the Vatican Museums, and the Trevi Fountain. What’s the best order to visit these attractions to minimize travel time? <|im_end|> Also, should I book tickets in advance for these places? <|im_end|>

TOVA

I’m planning a trip to Rome next month. I want to visit the Colosseum, the Vatican Museums, and the Trevi Fountain. What’s the best order to visit these attractions to minimize travel time? <|im_end|> Also, should I book tickets in advance for these places? <|im_end|>

Figure 7: All strategies compared on the qualitative example shown in Figure 1. The attention scores considered are from layer 12 head 0. Another qualitative example in Figure 11 and a failure case in Figure 8

864

865

866

867

Future Attention Importance

868

If a store offers a 20% discount on a jacket and the sale price is \$80, what was the original price? Please calculate the answer and let me know what you get. <|im_end|> The original price was \$100. Since the store took 20% off, the sale price represents the remaining 80% of the original price ($100\% - 20\% = 80\%$). To find the full price (100%), you divide the sale price by 0.80. <|im_end|>

873

874

KVP

875

If a store offers a 20% discount on a jacket and the sale price is \$80, what was the original price? Please calculate the answer and let me know what you get. <|im_end|> The original price was \$100. Since the store took 20% off, the sale price represents the remaining 80% of the original price ($100\% - 20\% = 80\%$). To find the full price (100%), you divide the sale price by 0.80. <|im_end|>

879

880

SnapKV

881

If a store offers a 20% discount on a jacket and the sale price is \$80, what was the original price? Please calculate the answer and let me know what you get. <|im_end|> The original price was \$100. Since the store took 20% off, the sale price represents the remaining 80% of the original price ($100\% - 20\% = 80\%$). To find the full price (100%), you divide the sale price by 0.80. <|im_end|>

885

886

Figure 8: A qualitative comparison of all strategies, similar to Figure 1. In this particular failure case, the attention scores from layer 10, head 0, show that our proposed KVP strategy struggles to fully capture the ground-truth future attention pattern.

889

890

891

892

893

894

895

896

897

898

899

900

901

902

903

904

905

906

907

908

909

910

911

912

913

914

915

916

917

KeyDiff

KNorm

If a store offers a 20% discount on a jacket and the sale price is \$80, what was the original price? Please calculate the answer and let me know what you get. <|im_end|> The original price was \$100. Since the store took 20% off, the sale price represents the remaining 80% of the original price ($100\% - 20\% = 80\%$). To find the full price (100%), you divide the sale price by 0.80. <|im_end|>

LagKV

Random

If a store offers a 20% discount on a jacket and the sale price is \$80, what was the original price? Please calculate the answer and let me know what you get. <|im_end|> The original price was \$100. Since the store took 20% off, the sale price represents the remaining 80% of the original price ($100\% - 20\% = 80\%$). To find the full price (100%), you divide the sale price by 0.80. <|im_end|>

TOVA

If a store offers a 20% discount on a jacket and the sale price is \$80, what was the original price? Please calculate the answer and let me know what you get. <|im_end|> The original price was \$100. Since the store took 20% off, the sale price represents the remaining 80% of the original price ($100\% - 20\% = 80\%$). To find the full price (100%), you divide the sale price by 0.80. <|im_end|>

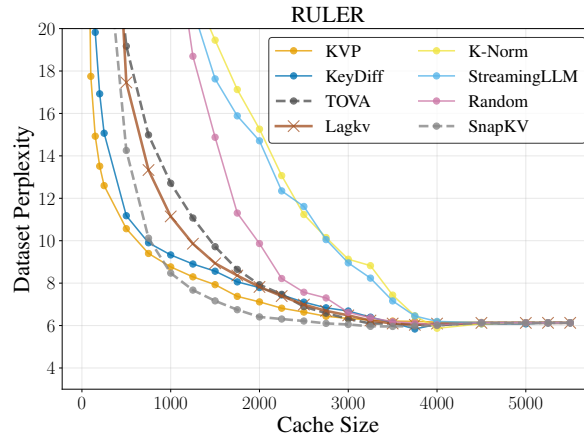
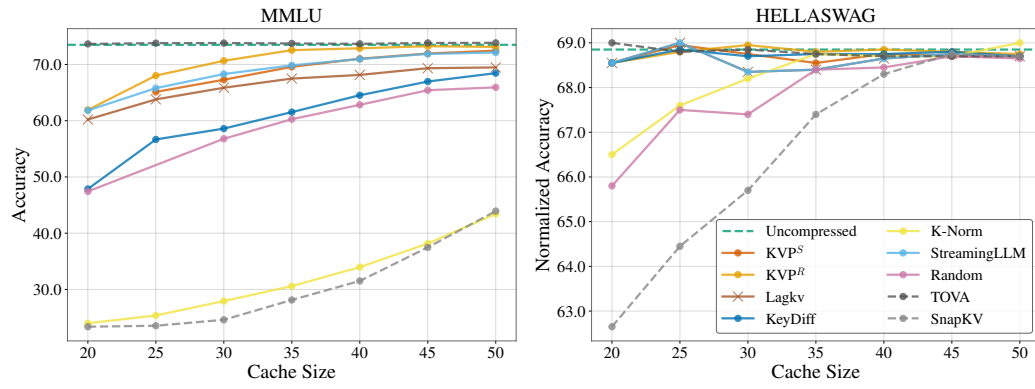


Figure 9: Perplexity (PPL) as a function of KV cache size. KVP achieves highly competitive perplexity, performing on par with or better than the leading baselines at most cache sizes and significantly outperforming other methods. This result is particularly notable given that RULER’s structure, which includes random sentences preceding a final question, heavily advantages methods that can isolate tokens relevant to that question.

918
919
920
921
922
923
924
925
926
927
928
929
930
931
932
933
934
935
936
937



950
951 Figure 10: (Left) Average test accuracy on MMLU and (Right) average normalized accuracy on
952 Hellaswag as a function of KV cache size. Higher is better.

953
954
955
956
957
958
959
960
961
962
963
964
965
966
967
968
969
970
971

Future Attention Importance
972
973 Each has been continuously updated since 1990. The *Model of Particulars* was developed in 1990, in the 10th year of the Canadian
974 *General University* (University). Since then, various updates have been provided by the *University's* teaching and
975 *Research* departments. The *Model of Particulars* is a general model of the *University's* teaching and research activities, and
976 *the 10th Model of Particulars* is the 10th update of the *Model of Particulars*. The *Model of Particulars* is a general model of
977 *the University's* teaching and research activities, and the *10th Model of Particulars* is the 10th update of the *Model of Particulars*.
978 *Each* has been continuously updated since 1990. The *Model of Particulars* was developed in 1990, in the 10th year of the Canadian
979 *General University* (University). Since then, various updates have been provided by the *University's* teaching and
980 *Research* departments. The *Model of Particulars* is a general model of the *University's* teaching and research activities, and
981 *the 10th Model of Particulars* is the 10th update of the *Model of Particulars*. The *Model of Particulars* is a general model of
982 *the University's* teaching and research activities, and the *10th Model of Particulars* is the 10th update of the *Model of Particulars*.
983 *Each* has been continuously updated since 1990. The *Model of Particulars* was developed in 1990, in the 10th year of the Canadian
984 *General University* (University). Since then, various updates have been provided by the *University's* teaching and
985 *Research* departments. The *Model of Particulars* is a general model of the *University's* teaching and research activities, and
986 *the 10th Model of Particulars* is the 10th update of the *Model of Particulars*. The *Model of Particulars* is a general model of
987 *the University's* teaching and research activities, and the *10th Model of Particulars* is the 10th update of the *Model of Particulars*.
988 *Each* has been continuously updated since 1990. The *Model of Particulars* was developed in 1990, in the 10th year of the Canadian
989 *General University* (University). Since then, various updates have been provided by the *University's* teaching and
990 *Research* departments. The *Model of Particulars* is a general model of the *University's* teaching and research activities, and
991 *the 10th Model of Particulars* is the 10th update of the *Model of Particulars*. The *Model of Particulars* is a general model of
992 *the University's* teaching and research activities, and the *10th Model of Particulars* is the 10th update of the *Model of Particulars*.
993 *Each* has been continuously updated since 1990. The *Model of Particulars* was developed in 1990, in the 10th year of the Canadian
994 *General University* (University). Since then, various updates have been provided by the *University's* teaching and
995 *Research* departments. The *Model of Particulars* is a general model of the *University's* teaching and research activities, and
996 *the 10th Model of Particulars* is the 10th update of the *Model of Particulars*. The *Model of Particulars* is a general model of
997 *the University's* teaching and research activities, and the *10th Model of Particulars* is the 10th update of the *Model of Particulars*.
998 *Each* has been continuously updated since 1990. The *Model of Particulars* was developed in 1990, in the 10th year of the Canadian
999 *General University* (University). Since then, various updates have been provided by the *University's* teaching and
999 *Research* departments. The *Model of Particulars* is a general model of the *University's* teaching and research activities, and
999 *the 10th Model of Particulars* is the 10th update of the *Model of Particulars*. The *Model of Particulars* is a general model of
999 *the University's* teaching and research activities, and the *10th Model of Particulars* is the 10th update of the *Model of Particulars*.

KVP

SnapKV

KeyDiff

KNorm

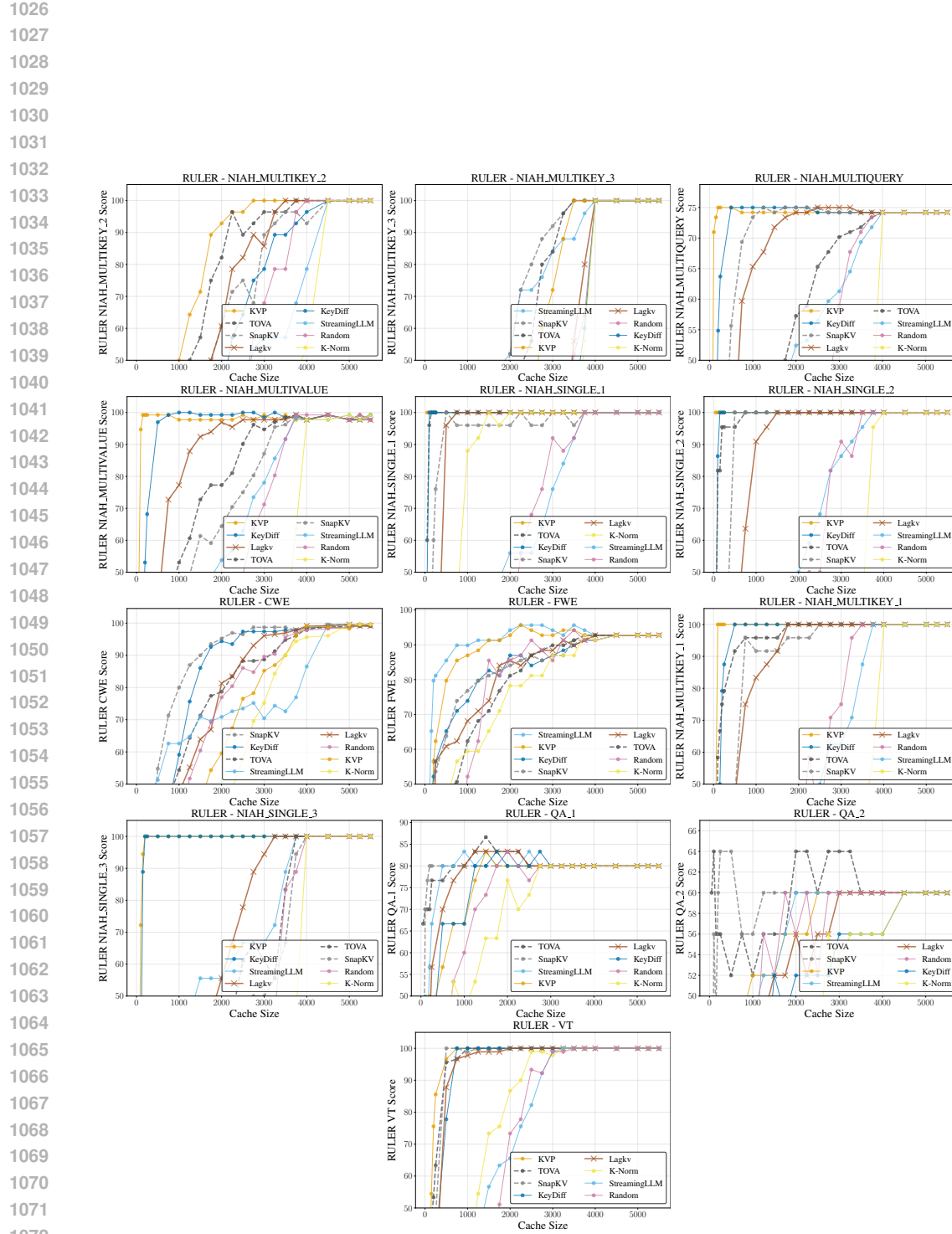
LagKV

Random

TOV

Roman times. The vicus of Tivoli appears to have per-

Figure 11: All strategies compared on a long qualitative example. The attention scores considered are from layer 19 head 0.

1073 Figure 12: Per-task accuracy on all RULER subtasks as a function of absolute KV cache size.
1074
1075
1076
1077
1078
1079

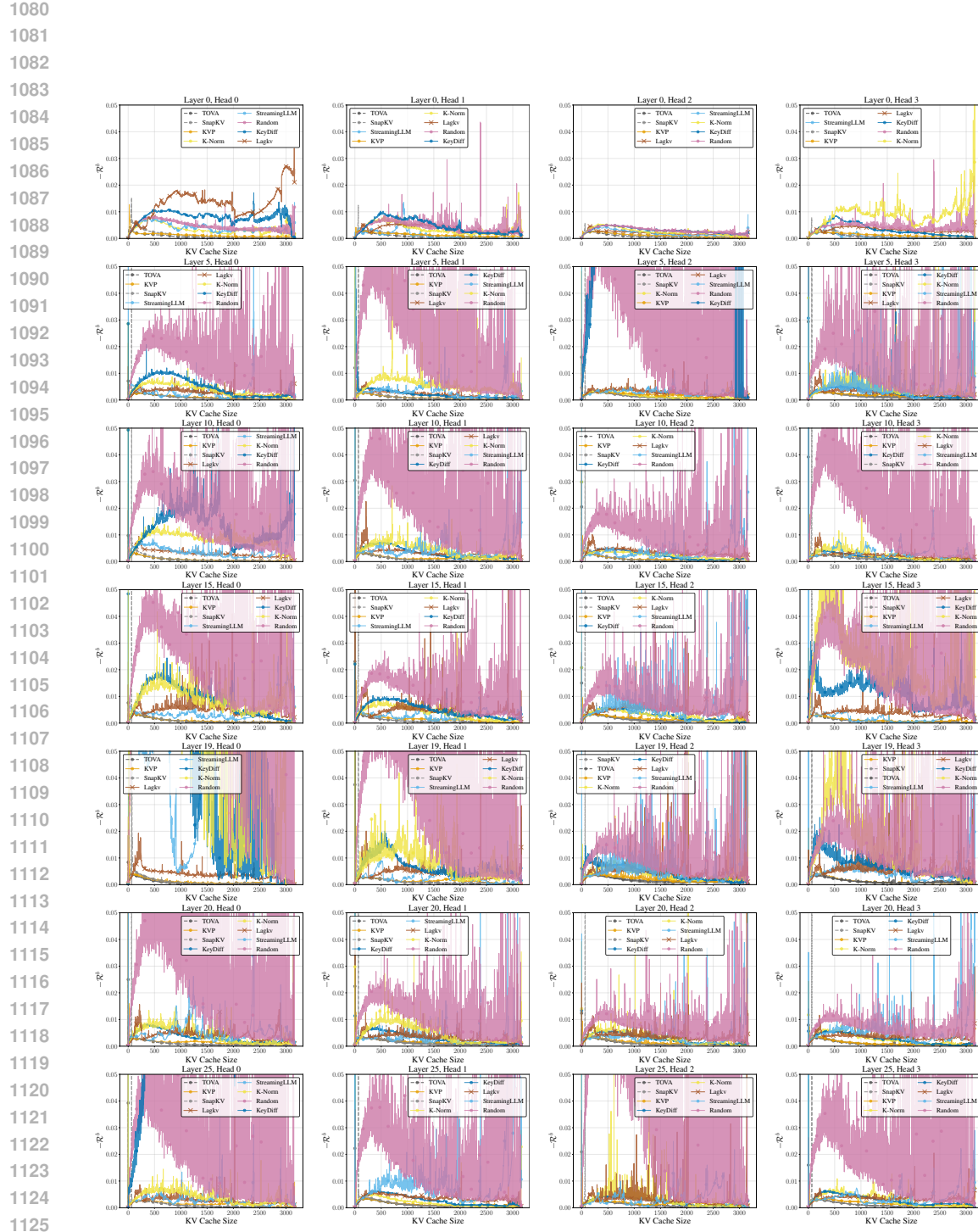


Figure 13: Cost ($-\mathcal{R}^b$) for all strategies across a selection of layers (rows) and all available heads (columns) on the OASST2 test set. The plots show that the relative performance of different strategies varies significantly across heads, highlighting the benefit of learning specialized per-head policies. Lower is better.

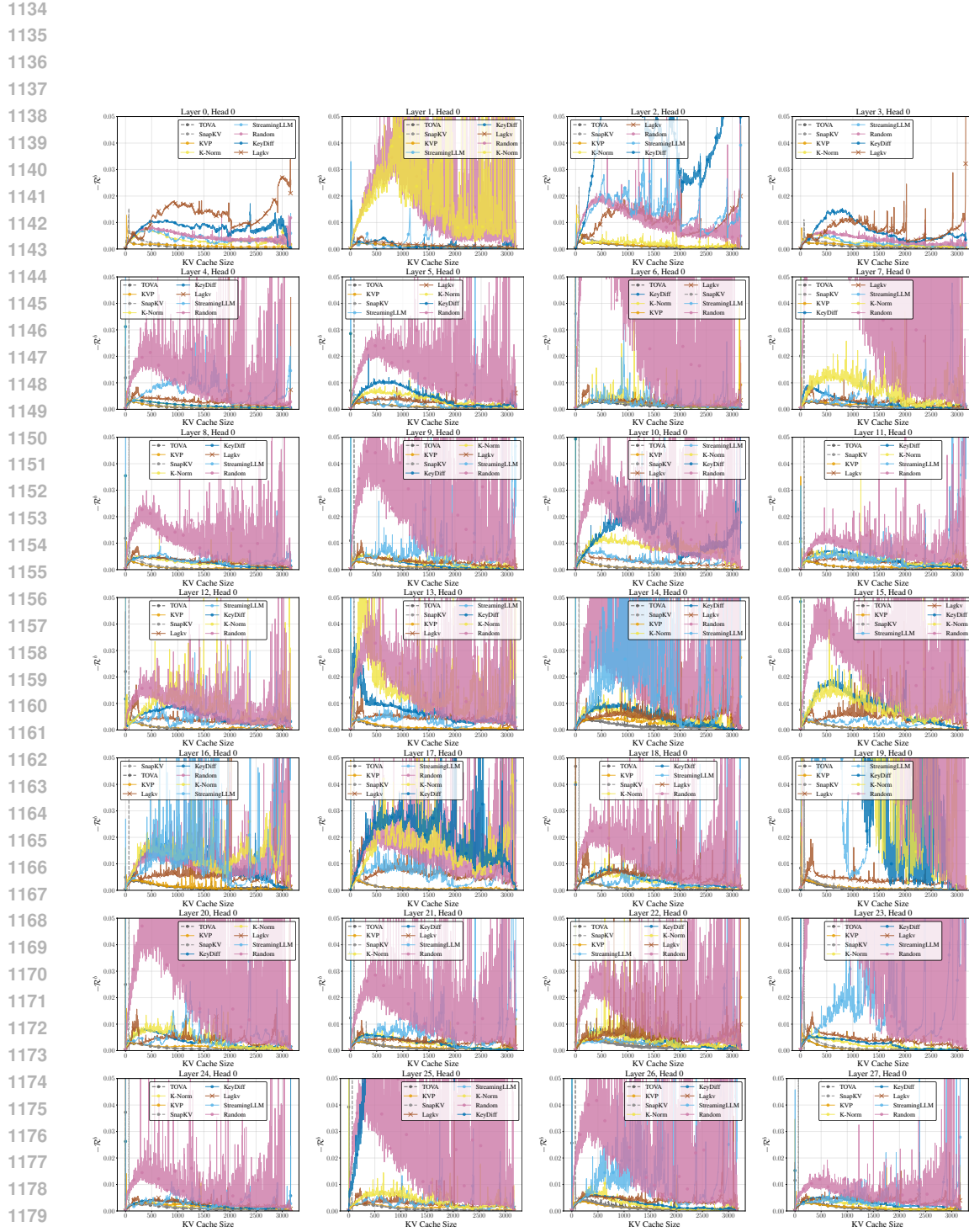


Figure 14: Cost ($-\mathcal{R}^b$) for all strategies on head 0 across all 28 layers of the model, evaluated on the OASST2 test set. This visualization shows how the effectiveness of different non attention-aware eviction heuristics changes with model depth, whereas the learned KVP policy remains consistently effective. Lower is better.